Relaxation of Spherical Micellar Systems of Styrene−Isoprene Diblock Copolymers. 2. Nonlinear Stress Relaxation Behavior

Hiroshi Watanabe,* Tomohiro Sato, and Kunihiro Osaki

Institute for Chemical Research, Kyoto University, Uji, Kyoto 611, Japan

Ming-Long Yao

Rheometric Scientific F. E., 2-19-6 Yanagibashi, Taito-ku, Tokyo 111, Japan

Received December 14, 1995; Revised Manuscript Received March 4, 1996[⊗]

ABSTRACT: Nonlinear stress relaxation after imposition of step strain γ (≤ 2) was examined for blends of styrene−isoprene (SI) diblock copolymers in a homopolyisoprene (hI) matrix. The blends contained spherical micelles with S cores and I corona. For most cases, the blends had no plasticity and exhibited complete relaxation. Fast and slow relaxation processes characterizing the linear viscoelastic behavior of the micelles (part 1) were observed also for nonlinear relaxation moduli $G(t,\gamma)$. For sufficiently small γ, $G(t,\gamma)$ agreed with the linear relaxation moduli evaluated from the G^* data of part 1. However, $G(t,\gamma)$ decreased for larger γ (mostly for $\gamma > 0.1$). This nonlinear damping was much more significant for the slow process than for the fast process. For quantitative analysis of the damping behavior, the *linear* viscoelastic relaxation time τ^* of the fast process was utilized to successfully separate the $G(t,\gamma)$ data into contributions from the fast and slow processes, $G_f(t,\gamma)$ and $G_s(t,\gamma)$, in the following way: At $t > 6\tau^*$ where the fast process had negligible contribution to $G(t,\gamma)$, $G_s(t,\gamma)$ were taken to be identical to $G(t,\gamma)$. By extrapolating those $G_s(t,\gamma)$ data to shorter time scales, $G_s(t,\gamma)$ were evaluated at $t < 6\tau^*$. $G_f(t,\gamma)$ were evaluated as $G(t,\gamma) - G_s(t,\gamma)$. For both $G_f(t,\gamma)$ and $G_s(t,\gamma)$, the terminal relaxation times were insensitive to γ and the time−strain separability held in respective terminal regions. This separability enabled us to define damping functions in those regions, $h_x(\gamma) = G_x(t,\gamma)/G_x(t)$ (x = f, s). For the fast process of the SI micelles, $h_f(\gamma)$ exhibited only modest γ dependence that was in good agreement with the dependence for homopolymer chains. This result indicated that the fast process corresponded to relaxation of *individual* corona I blocks, giving a strong support for the discussion of part 1. On the other hand, $h_s(\gamma)$ of concentrated micelles exhibited very strong γ dependence that was comparable, in both magnitudes and sensitivities to the I block concentration and molecular weight, with the dependence of the damping function $h_{C_{14}}(\gamma)$ obtained for solutions of SI in an I-selective solvent, *n*-tetradecane (C_{14}). Those solutions exhibited plasticity due to macrolattices of the micelles, and their nonlinearity was attributed to strain-induced changes in the micelle position. Thus, the similarity of $h_s(\gamma)$ and $h_{C_{14}}(\gamma)$ suggested that the slow process of the concentrated micelles in the SI/hI blends was related to the changes in the micelle position and the subsequent micelle diffusion, again supporting the discussion of part 1.

I. Introduction

In part 1 of this series of papers, we have examined the linear viscoelastic and dielectric relaxation behavior for micellar blends of styrene−isoprene (SI) diblock copolymers in a short, nonentangling homopolyisoprene (hI) matrix.[1] The micelles (with S cores and I corona) were found to exhibit fast and slow relaxation processes in their linear viscoelastic moduli and dielectric losses. The fast process was attributed to relaxation of individual corona I blocks, while for micelles entangled through their corona blocks the slow process was related to their diffusion.[1]

In this paper we further examine the mechanisms of the fast and slow processes of the SI micelles from a different point of view, nonlinearity of the stress relaxation behavior after imposition of large step strain, γ. The linear viscoelastic and dielectric responses examined in part 1 reflect the *equilibrium* thermal motion of the SI micelles and/or the corona I blocks. (Note that the linearity is generally observed for sufficiently small external stimuli, e.g., strain and electric field, that negligibly affect thermal motion involved in the system.) On the other hand, the nonlinear relaxation of the micellar blends should reflect the strain-induced, nonequilibrium motion involved in the fast and slow processes. Studies of such nonequilibrium relaxation processes are sometimes very useful for obtaining deeper insight for the dynamic phenomena, as evidenced from the success of the studies of nonlinear relaxation moduli $G(t,\gamma)$ of entangled homopolymer chains[2−7] that revealed the universal damping behavior of $G(t,\gamma)$ attributable to shrinkage of the chains. Since the fast process of the micellar blends is considered to reflect motion of individual I block chains while the slow process is not, a study of the nonlinear stress relaxation behavior of the blends is expected to give a key result for specifying mechanisms of those processes. Extensive data accumulated for nonlinear stress relaxation of homopolymer chains[2−8] should be useful for this specification.

On the basis of the above considerations, we have measured $G(t,\gamma)$ for the SI/hI micellar blends. For comparison, $G(t,\gamma)$ were measured also for SI solutions in an I-selective, low molecular weight solvent, *n*-tetradecane (C_{14}). These solutions exhibit plasticity due to macrolattices[9−12] of the SI micelles. Comparing the nonlinear behavior of the SI/hI blends with that of the SI/C_{14} and homopolymer systems, we discussed the relaxation mechanisms for the fast and slow processes of the blends. The results are presented in this paper.

II. Experimental Section

Molecular characteristics of the SI 43−86, SI 14−29, and I-4 samples and the method of the blend preparation were described in part 1. The sample code numbers indicate the block molecular weights in units of 1000. For the representative blends used in part 1, the 6 and 12.8 wt % blends of SI

[⊗] Abstract published in *Advance ACS Abstracts,* April 15, 1996.

S0024-9297(95)01844-4 CCC: $12.00

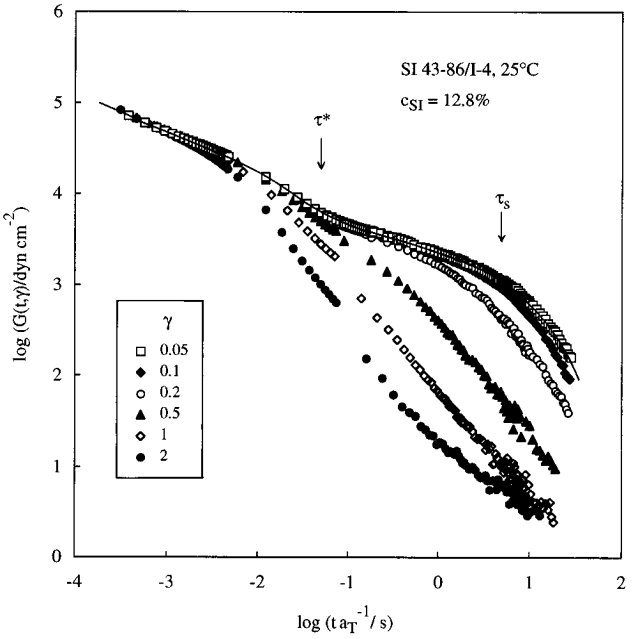

Figure 1. Nonlinear relaxation modulus $G(t,\gamma)$ at 25 °C for the 12.8 wt % SI 43-86/I-4 blend. The arrows indicate the relaxation times τ^* and τ_s for the fast and slow processes determined in the linear viscoelastic regime (part 1). The solid curve represents the linear relaxation modulus $G(t)$ determined from the G^* data of part 1.

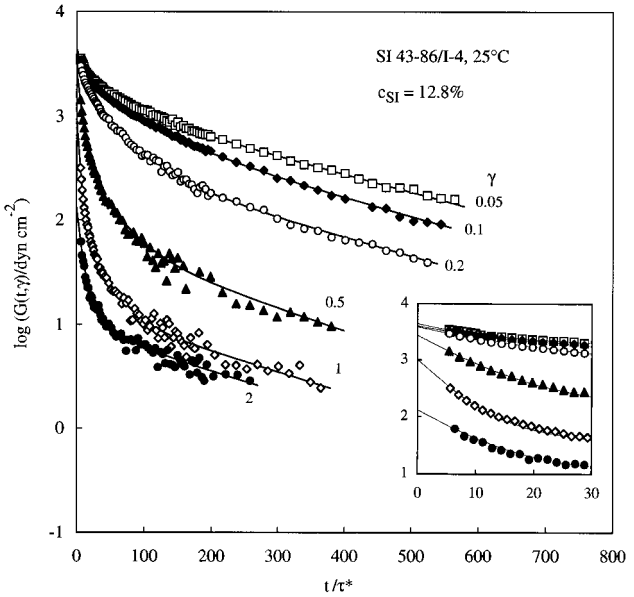

Figure 2. Semilogarithmic plots of $G(t,\gamma)$ at 25 °C for the 12.8 wt % SI 43-86/I-4 blend against reduced time, t/τ^*. The symbols are the same as in Figure 1. The data are shown at long time scales ($t > 6\tau^*$) where the fast process has negligible contribution to $G(t,\gamma)$. The solid curves indicate results of the fit for those data with a sum of 3−6 exponentially decaying terms. The inserted panel magnifies the plots at $6\tau^* < t < 30\tau^*$.

43-86 and the 15 and 25 wt % blends of SI 14-29, relaxational stresses $\sigma(t,\gamma)$ were measured over five decades of magnitudes after imposition of the step strain γ (=0.05−2) and the nonlinear relaxation moduli, $G(t,\gamma) = \sigma(t,\gamma)/\gamma$, were determined. Cone and plate geometry (of radius =1.25 cm and cone angle =0.1 rad) was used. To cover this wide range of $\sigma(t,\gamma)$, two rheometers of different dynamic ranges (RDAII and RFSII, Rheometrics) were used. The measurements were carried out at 25 °C and lower temperatures (+5 and −25 °C) to cover sufficiently wide ranges of time where the fast and slow relaxation processes described in part 1 were observed. The time−temperature shift factors a_T for the linear G^* data (part 1) were used to reduce the $G(t,\gamma)$ data at +5 and −25 °C to a reference temperature, 25 °C.

Spherical micelles with S cores and I corona were formed in the above four blends. As explained in part 1, the I blocks of neighboring micelles are entangled in the 12.8 wt % blend of SI 43-86 and the 25 wt % blends of SI 14-29, but not in the 6 wt % blend of SI 43-86 and the 15 wt % blends of SI 14-29. Among these blends, the 6 and 12.8 wt % blends of SI 43-86 and the 15 wt % blend of SI 14-29 exhibited terminal relaxation in both linear and nonlinear regimes, indicating that the micelles were randomly dispersed in those blends. On the other hand, in the linear regime the 25 wt % blend of SI 14-29 was essentially elastic and exhibited no terminal relaxation (cf. part 1), suggesting that the micelles formed a macrolattice in this blend. Thus, this blend was expected to exhibit plastic behavior for large γ. For comparison with this expected behavior, nonlinear stress relaxation measurements were carried out at 25 °C also for moderately concentrated micellar solutions of the SI samples in *n*-tetradecane (C_{14}). C_{14} is an I-selective solvent, and previous work[9−12] on similar solutions confirmed that the solutions have plasticity due to the macrolattices of the micelles.

III. Results and Discussion

III-1. Overview. For the 12.8 wt % SI 43-86/I-4 blend at 25 °C, Figure 1 shows the nonlinear relaxation modulus $G(t,\gamma)$ obtained for γ = 0.05−2. The arrows indicate *linear* viscoelastic relaxation times for the fast and slow processes, τ^* and τ_s (cf. part 1).[1] The solid curve represents the relaxation modulus in the linear regime, $G(t)$, that was evaluated from the G' and G'' data of part 1 by the method of Ninomiya and Ferry,[13]

$$G(t) = [G'(\omega) - 0.4G''(0.4\omega) + 0.014G''(10\omega)]_{\omega=1/t} \quad (1)$$

As noted in Figure 1, fast and slow relaxation processes are observed for $G(t,\gamma)$ in the entire range of γ. Since the matrix I-4 chains have relaxed at the time scales examined, both processes are exclusively attributed to relaxation of the micelles. For the smallest γ (=0.05), $G(t,\gamma)$ coincides with $G(t)$ in the entire range of time and the linear viscoelastic behavior is detected also in the stress relaxation experiments. However, $G(t,\gamma)$ deviates downward from $G(t)$ for larger γ. Clearly, this nonlinear *damping* of the modulus is much more significant for the slow process than for the fast process. This large difference demonstrates differences in the mechanisms of the two processes.

Figure 2 shows semilogarithmic plots of the data of Figure 1. The $G(t,\gamma)$ data (symbols) at long time scales ($t > 6\tau^*$) are plotted against a reduced time, t/τ^*. The solid curves indicate results of fit for those data, as explained later in section III-2. *At sufficiently long time scales*, the log $G(t,\gamma)$ data depend linearly on t/τ^* and thus $G(t,\gamma)$ decays as a single exponential function of t. This exponential decay characterizes the terminal regions for the slow process, and the time constant for the decay is identical to the terminal relaxation time of that process. As noted in Figure 2, this relaxation time is insensitive to γ. (Since this feature of the slow process is not easily noted from the double-logarithmic plots in Figure 1, the semilogarithmic plots have been shown here.)

Here, we have to emphasize that the nonlinear damping behavior seen in Figures 1 and 2 is *not* due to strain-induced rupture of the S cores, as evidenced from a fact that the $G(t,\gamma)$ data for the smallest γ (=0.05) were reproduced after a relaxation experiment for the largest γ (=2). This was the case also for the other SI/I-4 blends

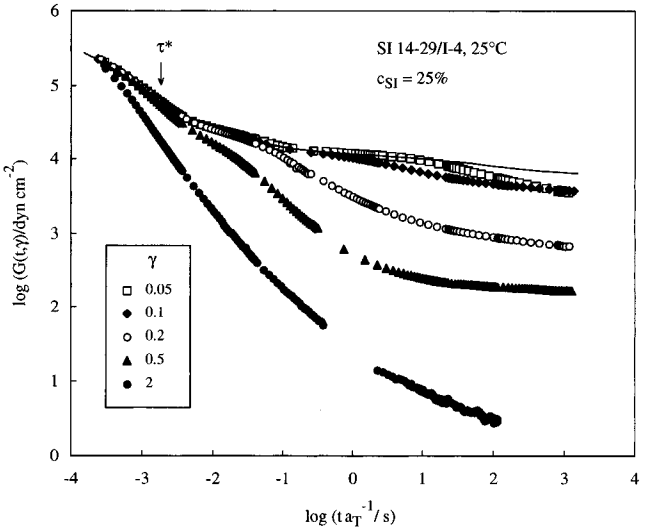

Figure 3. Nonlinear relaxation modulus $G(t,\gamma)$ at 25 °C for the 25 wt % SI 14-29/I-4 blend. The arrow indicates the relaxation time τ^* for the fast process determined in the linear viscoelastic regime (part 1). The solid curve represents the linear relaxation modulus $G(t)$ determined from the G^* data of part 1.

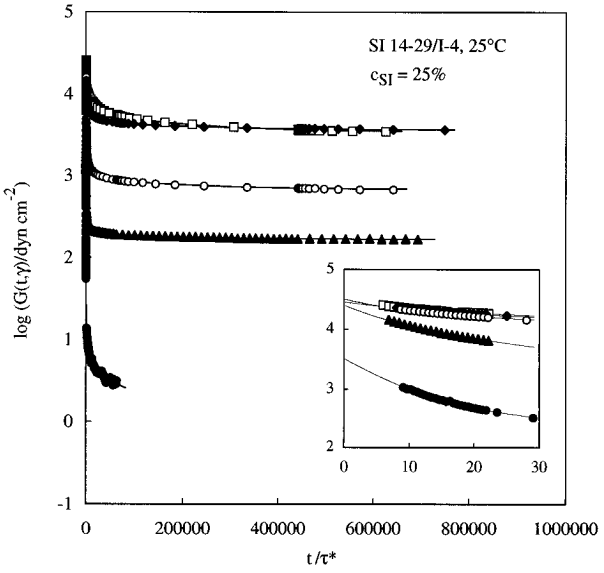

Figure 4. Semilogarithmic plots of $G(t,\gamma)$ at 25 °C for the 25 wt % SI 14-29/I-4 blend against reduced time, t/τ^*. The symbols are the same as in Figure 3. The data are shown at long time scales ($t > 6\tau^*$) where the fast process has a negligible contribution to $G(t,\gamma)$. The solid curves indicate results of the fit for those data with a sum of 3−6 exponentially decaying terms. (For $\gamma \leq 0.5$, one of those terms has infinite relaxation time and corresponds to the unrelaxed modulus.) The inserted panel magnifies the plots at $6\tau^* < t < 30\tau^*$.

examined in this study. (Note that all $G(t,\gamma)$ data were obtained at $T \leq 25$ °C where the S cores were glassy and rigid. Those cores were embedded in the soft I matrices and could not be broken by the rather modest strain ($\gamma \leq 2$) applied to the blends.)

For the 6 wt % SI 43-86/I-4 and 15 wt % SI 14-29/I-4 blends exhibiting terminal relaxation, the nonlinear features were similar to those seen in Figures 1 and 2: These blends exhibited the fast and slow processes in $G(t,\gamma)$ and had the γ-insensitive terminal relaxation times. The slow process exhibited much stronger damping as compared to the fast process, and the linear relaxation behavior was observed only for $\gamma \leq 0.1$. Somewhat different features were observed for the 25 wt % SI 14-29/I-4 blend that behaved elastically and exhibited no terminal relaxation in the linear viscoelastic regime. Figures 3 and 4 show the nonlinear behavior of this blend in the double-logarithmic and semilogarithmic scales. The solid curve in Figure 3 indicates the linear relaxation modulus $G(t)$ evaluated with eq 1. As in Figure 2, the $G(t,\gamma)$ data at $t > 6\tau^*$ are plotted against t/τ^* in Figure 4 (symbols).

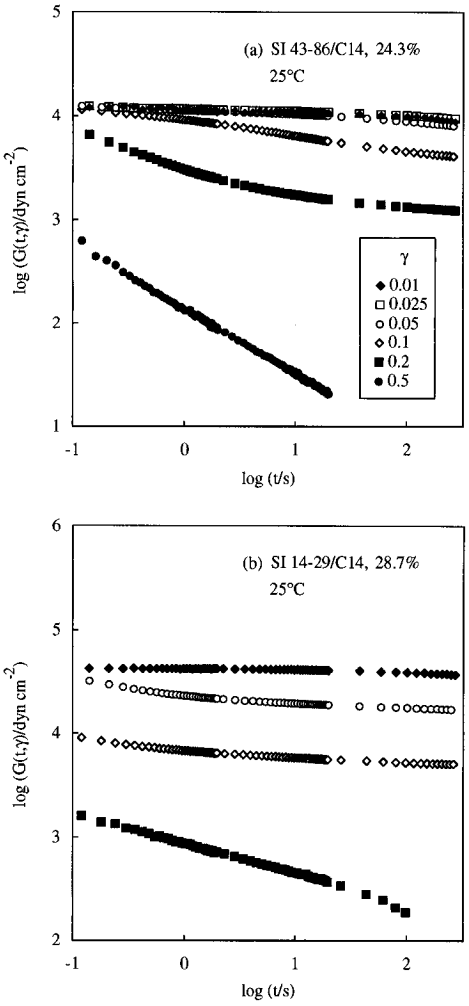

Figure 5. Nonlinear relaxation moduli $G(t,\gamma)$ at 25 °C for the *n*-tetradecane solutions of (a) SI 43-86 (24.3 wt %) and (b) SI 14-29 (28.7 wt %).

In Figure 3, we note agreements between $G(t,\gamma)$ obtained for $\gamma = 0.05$ and the linear $G(t)$ except at the long time end. We also note that the fast process observed at around τ^* (arrow) exhibits only modest nonlinear damping. These features of the 25 wt % SI 14-29/I-4 blend are similar to those found for the other blends (cf. Figure 1). However, Figures 3 and 4 also indicate that the 25 wt % SI 14-29/I-4 blend does not exhibit terminal relaxation but has a plateau in $G(t,\gamma)$ at long time scales for $\gamma \leq 0.5$. Even for γ as small as 0.05, this plateau is considerably lower than that of $G(t)$ and the nonlinear damping is observed (cf. Figure 3). This damping is stronger than that for the slow process of the other blends exhibiting complete relaxation (cf. Figures 1 and 2). Finally, for larger γ (=2), the 25 wt % SI 14-29/I-4 blend appears to flow.

Figure 5 shows $G(t,\gamma)$ for *n*-tetradecane (C_{14}) solutions of (a) SI 43-86 (24.3 wt %) and (b) SI 14-29 (28.7 wt %). C_{14} is an I-selective solvent, and the solutions have plasticity due to macrolattices[9−12] of the micelles (with S cores and I corona). The concentration (28.7 wt %) in

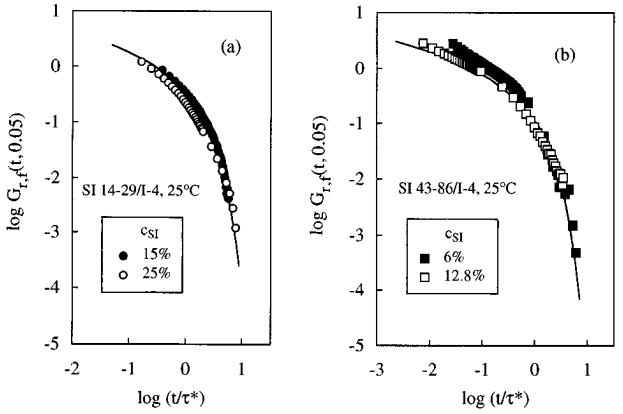

Figure 6. Comparison of the reduced moduli $G_{r,f}(t,0.05)$ for the fast process of the SI/I-4 blends (symbols) with the reduced, *linear* relaxation moduli $G_{r,star}(t)$ for star-hI chains having $M_a \cong M_{bI}$ (curves): (a) SI 14-29 blends (M_{bI} = 28.8K) and star-hI with M_a = 36.7K; (b) SI 43-86 blends (M_{bI} = 85.8K) and star-hI with M_a = 95K. $G_{r,star}(t)$ is close to the reduced, *linear* modulus for the fast process, $G_{r,f}(t)$.

the SI 14-29 solution (part b) was chosen so that the I blocks in the I/C_{14} matrix had the same concentration c_{bI} (in mass/volume unit) as that in the matrix of the 25 wt % SI 14-29/I-4 blend. The solutions are expected to exhibit the fast process similar to those seen in Figures 1 and 3. However, this process is too fast to be detected in our experimental window, because a segmental friction for the I blocks is much smaller in the low molecular weight solvent C_{14} than in the polymeric I-4 matrix. Thus, the behavior seen in Figure 5 corresponds to that of the SI blends at long time scales.

As seen in Figure 5, the SI/C_{14} solutions exhibit nonlinear features similar to that for the 25 wt % SI 14-29/I-4 blend: The solutions do not flow for small γ but have a plateau in $G(t,\gamma)$ at long time scales for relatively small γ. This plateau exhibits strong damping even for γ as small as 0.05, and the linear viscoelastic behavior is observed only for very small γ ($\leq$0.025 in part a). Finally, the solutions appear to flow for large γ. These features seem to be characteristic of micellar systems having macrolattices. As explained later in section III-4, similarities between the SI/C_{14} solutions and the SI/I-4 blends give us a clue for discussing the mechanism of the slow process of the blends.

III-2. Separation of Nonlinear Moduli for the Fast and Slow Processes. Quantitative analysis for the fast and slow processes should be carried out for the nonlinear relaxation moduli for respective processes, $G_f(t,\gamma)$ and $G_s(t,\gamma)$. For this purpose, we used the *linear* viscoelastic relaxation time τ^* of the fast process determined in part 1 and evaluated $G_f(t,\gamma)$ and $G_s(t,\gamma)$ in the following way.

In general, relaxation processes may be accelerated but not retarded by a large strain: For example, relaxation of thixotropic dispersion systems is usually accelerated by the strain. Thus, we may naturally consider that in the entire range of γ (including the nonlinear regime) the fast process is completed at time scales sufficiently longer than τ^*. In other words, $G(t,\gamma)$ is identical to $G_s(t,\gamma)$ of the slow process at those time scales. Specifically, we chose a time scale, $t > 6\tau^*$: Since $G_f(t,\gamma)$ of the fast process should be expressed as a sum of exponential terms with characteristic decay times $\leq\tau^*$, $G_f(t,\gamma)$ decays by a factor $<\exp(-6) = 0.0025$ at $t > 6\tau^*$ and its contribution to $G(t,\gamma)$ should be negligible at those t. Thus, we equated $G(t,\gamma)$ and $G_s(t,\gamma)$ at $t > 6\tau^*$.

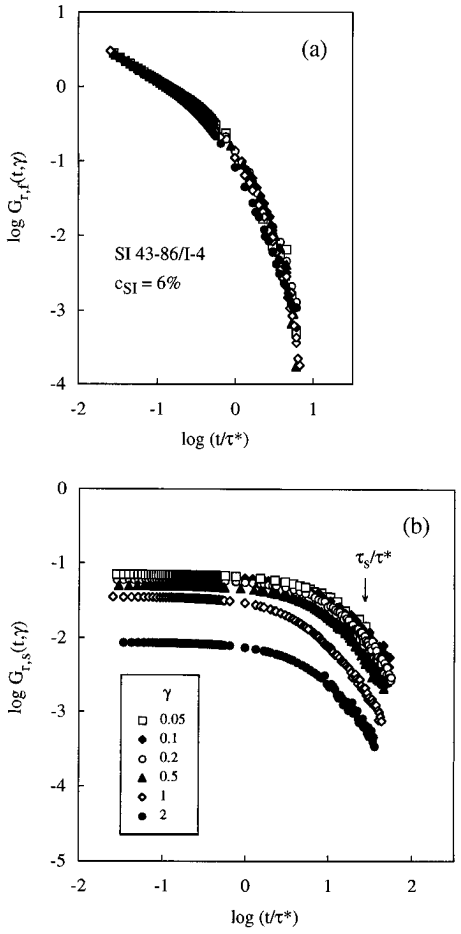

Figure 7. Reduced nonlinear relaxation moduli $G_{r,f}(t,\gamma)$ and $G_{r,s}(t,\gamma)$ for the fast and slow processes of the 6 wt % SI 43-86/I-4 blend at 25 °C.

The $G(t,\gamma)$ data at $t > 6\tau^*$ ($=G_s(t,\gamma)$) were fitted with a sum of exponentially decaying terms. In Figures 2 and 4, the solid curves indicate the results of the fit. A good fit was achieved with 3−6 terms of characteristic times $\geq 5\tau^*$. (The largest in those times is the terminal relaxation time mentioned for Figure 2.) For the 25 wt % SI 14-29/I-4 blend (Figure 4), one of the fitting terms used for $\gamma \leq 0.5$ was a constant term (i.e., having infinite relaxation time) that represented the unrelaxed modulus. Extrapolating the fitting function thus obtained to $t = 0$ (cf. inserted panels in Figures 2 and 4), we evaluated $G_s(t,\gamma)$ at $t < 6\tau^*$ and $G_f(t,\gamma) = G(t,\gamma) - G_s(t,\gamma)$.

The results of Figures 1 and 3 are useful for testing the accuracy of the above evaluation: As seen there, $G(t, 0.05)$ obtained for $\gamma = 0.05$ agrees with the linear relaxation modulus $G(t)$ at time scales of the fast process. Thus, the corresponding $G_f(t, 0.05)$ has to coincide with the linear modulus $G_f(t)$ for this process. As shown in part 1, the dynamic moduli of bulk star-hI reduced by the arm molecular weight M_a and density ρ_I, $G_{r,star}^*$, are very close to the similarly reduced G_r^* of the SI blends in the fast relaxation regime. Consequently, the reduced, linear relaxation modulus of star-hI, $G_{r,star}(t) = [M_a/\rho_I RT]G_{star}(t)$ should be close to that for the fast process of the blends, $G_{r,f}(t) = [M_{bI}/c_{bI}RT]$-$G_f(t)$. Here, $G_{star}(t)$ is the linear modulus evaluated from G_{star}^* (part 1) by eq 1. Thus, we compared $G_{r,star}(t)$ and $G_{r,f}(t, 0.05) = [M_{bI}/c_{bI}RT]G_f(t, 0.05)$, with $G_f(t, 0.05)$ being evaluated with the above extrapolation method. The results are shown in Figure 6 where the reduced moduli are plotted against reduced times, t/τ^* (for the blends) and t/τ_{star} (for star-hI). Good agreements are observed

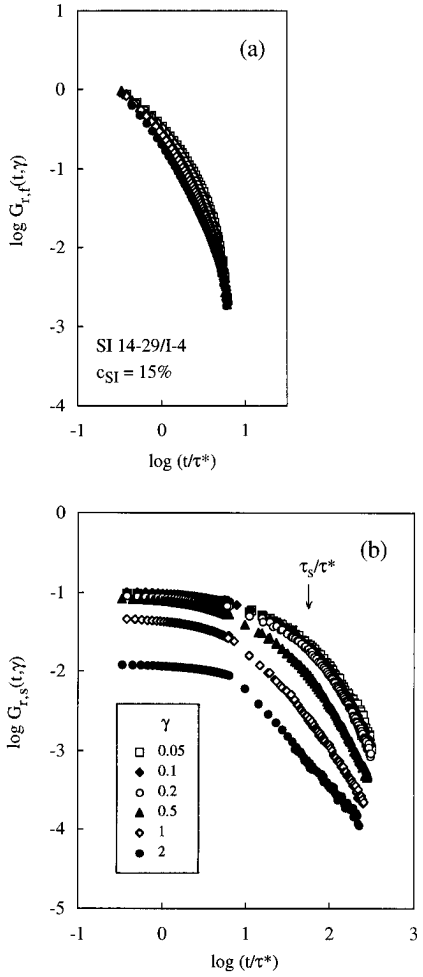

Figure 8. Reduced nonlinear relaxation moduli $G_{r,f}(t,\gamma)$ and $G_{r,s}(t,\gamma)$ for the fast and slow processes of the 15 wt % SI 14-29/I-4 blend at 25 °C.

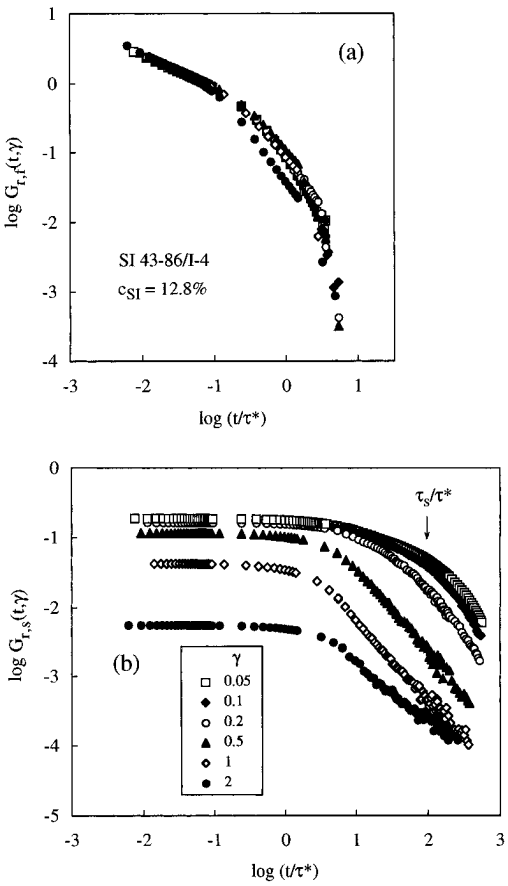

Figure 9. Reduced nonlinear relaxation moduli $G_{r,f}(t,\gamma)$ and $G_{r,s}(t,\gamma)$ for the fast and slow processes of the 12.8 wt % SI 43-86/I-4 blend at 25 °C.

for $G_{r,f}(t, 0.05)$ (symbols) and $G_{r,star}(t)$ ($=G_{r,f}(t)$; solid curves), indicating that $G_f(t,\gamma)$ and $G_s(t,\gamma)$ are successfully evaluated with that method.

Figures 7−10 examine γ dependence of the reduced relaxation moduli for the fast and slow processes of the SI blends, $G_{r,x}(t,\gamma) = [M_{bI}/c_{bI}RT]G_x(t,\gamma)$ with x = f and s. The arrows in part b indicate the *linear* viscoelastic relaxation time τ_s of the slow process (cf. part 1). Clearly, the nonlinear damping behavior is much more significant for the slow process (part b) than for the fast process (part a). We also note that the magnitude of damping for the fast process is rather insensitive to M_{bI} and c_{bI} while that for the slow process is strongly dependent on M_{bI} and c_{bI}. These results again demonstrate differences in the relaxation mechanisms of the two processes.

III-3. Mechanism for the Fast Process. As noted for part a of Figures 7−10, the fast processes of the SI micellar blends exhibit only modest damping behavior. Close inspection of those figures suggests that the mode distribution of $G_f(t,\gamma)$ (observed as the shape of the $G_f(t,\gamma)$ curves) is insensitive to γ at long time scales. From this result, we expect that the time−strain separability holds for $G_f(t,\gamma)$ at long time scales. This expectation is examined in Figure 11 where the $G_{r,f}(t,\gamma)$ curves are vertically shifted and superposed with each other at long time scales (symbols). For respective blends, $G_f(t, 0.05)$ obtained for $\gamma = 0.05$ agrees with the linear $G_f(t)$ (cf. Figure 6). Thus, $G_f(t, 0.05)$ was used as a reference for the shift. The solid curves represent the reduced modulus of the star-hI, $G_{r,star}(t)$ (cf. Figure 6).

As seen in Figure 11, good superposition is achieved for the $G_{r,f}(t,\gamma)$ curves of respective SI blends at $t \geq \tau^*/2$ and validity of the time−strain separability is confirmed. This fact enables us to define a damping function for the fast process,

$$h_f(\gamma) = [G_{r,f}(t,\gamma)/G_{r,f}(t)]_{t\geq\tau^*/2} \qquad (2)$$

Figure 12 shows the γ dependence of h_f for the micellar blends (large unfilled symbols). The small filled symbols indicate the damping function $h(\gamma)$ reported for entangled homopolystyrene (hS) solutions,[2−4] and the solid curve is the prediction of the Doi−Edwards theory for shrinkage of a chain trapped in a tube.[7] Those $h(\gamma)$ data are well described by the Doi−Edwards theory.

It is well-known that entangled homopolymer chains exhibit (almost) universal, characteristic γ dependence of $h(\gamma)$ that is insensitive to the concentration, molecular weight, and chemical and topological (linear/star) structures of the chain. This characteristic dependence is seen in Figure 12 also for the SI 43-86 (12.8 wt %) and SI 14-29 (25 wt %) blends in which the neighboring micelles are entangled through their corona I blocks: $h_f(\gamma)$ of these blends having different c_{bI} and M_{bI} are indistinguishable and in good agreement with $h(\gamma)$ for the hS chains. This fact suggests that the nonlinear damping mechanism for the fast processes of the entangled blends is the same as the mechanism for homopolymers, shrinkage of *individual* chains along the tube axis (coarse-grained chain contour).[2−7] Thus, also in the linear viscoelastic regime, the fast process of the micelles is naturally attributed to motion (or relaxation)

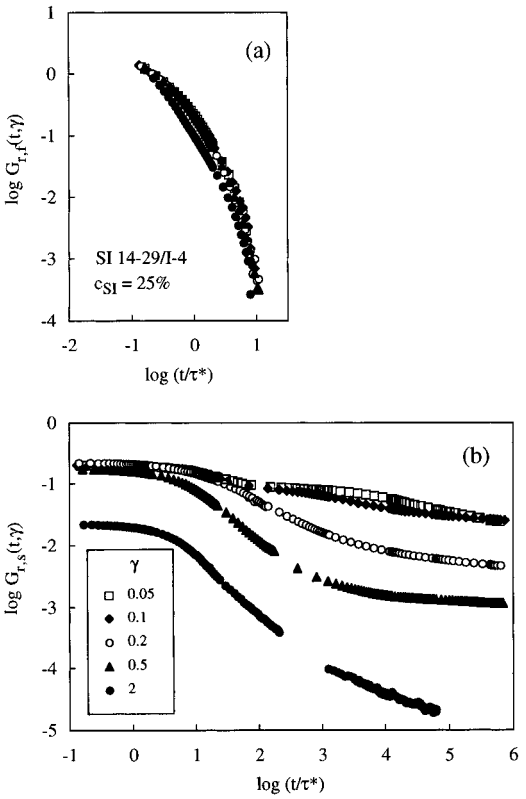

Figure 10. Reduced nonlinear relaxation moduli $G_{r,f}(t,\gamma)$ and $G_{r,s}(t,\gamma)$ for the fast and slow processes of the 25 wt % SI 14-29/I-4 blend at 25 °C.

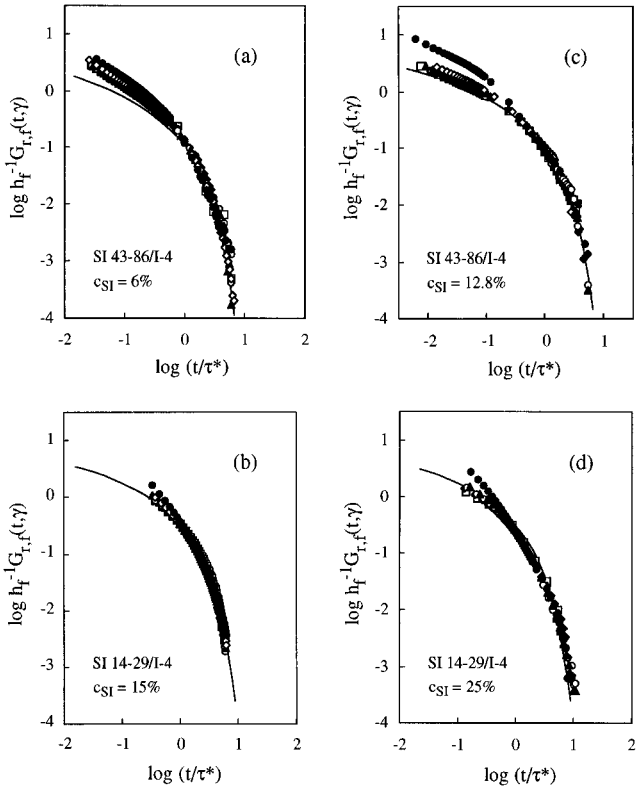

Figure 11. Examination of the time−strain separability of $G_{r,f}(t,\gamma)$ at 25 °C for the SI/I-4 blends as indicated. For respective blends, the $G_{r,f}(t,\gamma)$ curves are vertically shifted by factors $h_f(\gamma)$ to achieve the best superposition at long time scales. The curve obtained for the smallest γ (=0.05) was used as the reference for the shift. The symbols are the same as those used in Figures 7−10. The solid curves indicate $G_{r,star}(t)$ for the star-hI chains (cf. Figure 6).

of *individual* corona I blocks, giving a strong support for the molecular assignment of part 1.

In Figure 12, we also note that the damping at the largest γ (=2) is somewhat weaker for the nonentangled blends (6 wt % blend of SI 43-86 and 15 wt % blend of SI 14-29) than for the entangled blends. Similarly weak damping has been found for relaxation of nonentangled homopolymer chains.[8] Thus, the nonlinear behavior of those nonentangled blends also supports the assignment of part 1 for the fast process.

III-4. Mechanism for the Slow Process. For SI/I-4 blends exhibiting complete relaxation, $G(t,\gamma)$ (=$G_s(t,\gamma)$ at $t > 6\tau^*$) have γ-insensitive terminal relaxation times (cf. Figure 2). From this result, validity of the time−strain separability is expected for $G_s(t,\gamma)$ at long time scales. We vertically shifted and superposed the $G_{r,s}(t,\gamma)$ curves to examine this expectation. The results are shown in Figure 13. In the entire range of time, the 6 and 12.8 wt % blends of SI 43-86 and the 15% blend of SI 14-29 exhibited linear relaxation behavior for γ = 0.05 (cf. Figure 1) and $G_{r,s}(t, 0.05)$ gave the reduced, linear modulus for the slow process $G_{r,s}(t)$. Thus, in parts a−c of Figure 13, $G_{r,s}(t, 0.05)$ is used as a reference for the shift for those blends. On the other hand, the 25 wt % blend of SI 14-29 exhibited nonlinear damping of the plateau in $G_{r,s}(t,\gamma)$ at long time scales even for γ as small as 0.05 (cf. Figure 3). Thus, as we did for $G(t,\gamma)$, we evaluated the linear $G_{r,s}(t)$ of this blend from the $G(t)$ data shown in Figure 3. In part d of Figure 13, this $G_{r,s}(t)$ curve is used as the reference (solid curve) on which the nonlinear $G_{r,s}(t,\gamma)$ curves (symbols) were superposed at long time ends.

As seen in Figure 13, good superposition is achieved for the $G_{r,s}(t,\gamma)$ curves of respective SI blends at long time scales. This feature is qualitatively similar to that of the fast process. However, changes in the relaxation

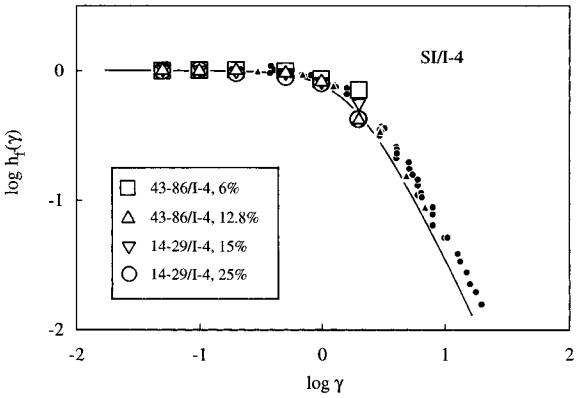

Figure 12. Damping function $h_f(\gamma)$ for the fast process of the SI micellar blends at 25 °C (large unfilled symbols). The small filled circles indicate the damping function $h(\gamma)$ for entangled, linear homopolystyrene (hS) solutions[2,4] (of M = 4.48M and 8.24M and c = 0.02−0.08 g/cm^3), and the small filled triangles indicate $h(\gamma)$ for entangled, 4-arm star hS solutions[3,4] (of M_a = 184K, 310K, and 662K and c = 0.08−0.3 g/cm^3). The solid curve represents the prediction of the Doi−Edwards theory (without the independent alignment approximation).[7]

mode distribution with γ (observed as changes in the shape of the $G_r(t,\gamma)$ curves) are much more significant for the slow process than for the fast process (cf. Figures 11 and 13). This result again indicates the difference between the two processes.

For the three SI/I-4 blends exhibiting terminal relaxation, we used the data of Figure 13 at $t \geq \tau_s$ (the linear viscoelastic relaxation time for the slow process) to evaluate a damping function for this process,

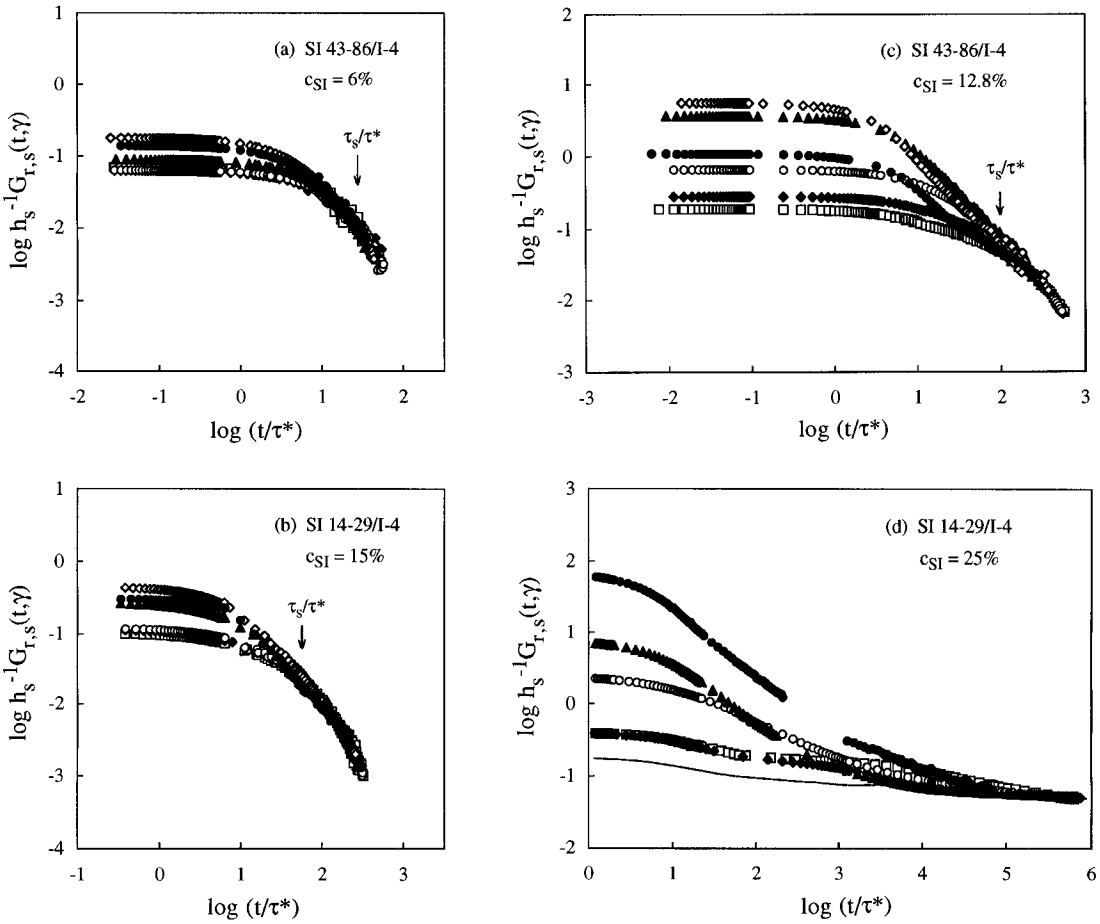

Figure 13. Examination of the time−strain separability of $G_{r,s}(t,\gamma)$ at 25 °C for the SI/I-4 blends as indicated. For the respective blends, the $G_{r,s}(t,\gamma)$ curves are vertically shifted by factors $h_s(\gamma)$ to achieve the best superposition at long time scales. $G_{r,s}(t,0.05)$ obtained for the smallest γ (=0.05) is used as the reference for the shift in parts a−c, while $G_{r,s}(t)$ evaluated from $G(t)$ data is used as the reference in part d (solid curve). The symbols are the same as those used in Figures 7−10.

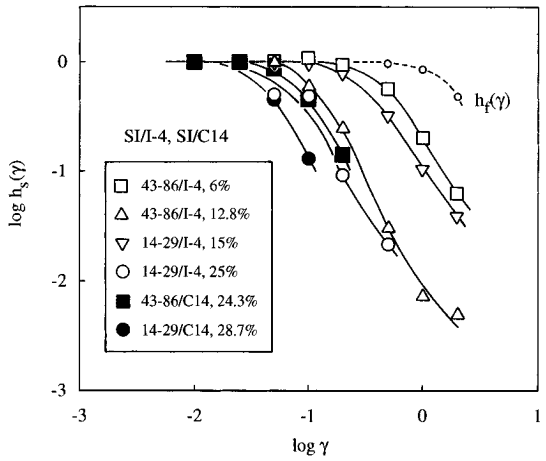

Figure 14. Damping function $h_s(\gamma)$ for the slow process of the SI micellar blends at 25 °C (large unfilled symbols). The large filled symbols indicate the damping function $h_{C_{14}}(\gamma)$ for the two SI/C_{14} solutions (cf. Figure 5). For comparison, $h_f(\gamma)$ for the fast process of the entangled SI micelles is shown with the small circles.

$$h_s(\gamma) = [G_{r,s}(t,\gamma)/G_{r,s}(t)]_{t\geq\tau_s} \qquad (3)$$

For the 25 wt % SI 14-29 blend exhibiting the plateau in $G_{r,s}(t,\gamma)$ even at the long time end (Figure 13d), we evaluated $h_s(\gamma)$ from its $G_{r,s}$ data at $t/\tau^* = 10^5-10^6$. Figure 14 shows the γ dependence of h_s for those SI blends (large unfilled symbols). The large filled symbols indicate the damping function $h_{C_{14}}(\gamma)$ for the two SI/C_{14} solutions (cf., Figure 5) that was defined for the long time ends of the $G(t,\gamma)$ curves (as done for the 25 wt % SI 14-29 blend). For these solutions, $G(t,0.01)$ obtained for $\gamma = 0.01$ was used as the reference for the shift. For comparison, $h_f(\gamma)$ for the fast process of the entangled SI micelles are shown with the small circles.

In Figure 14, we find that the γ dependence of $h_s(\gamma)$ largely changes with the I block molecular weight and concentration, M_{bI} and c_{bI}. Similar features are seen for $h_{C_{14}}(\gamma)$ but not for $h_f(\gamma)$ (cf. Figure 12). This result and the large differences in the γ dependence of $h_s(\gamma)$ and $h_f(\gamma)$ allow us to conclude that the slow process of the SI micelles does not reflect the relaxation of *individual* I blocks.

In Figure 14, we also note that magnitudes of $h_s(\gamma)$ for the concentrated SI/I-4 blends are comparable to those of $h_{C_{14}}(\gamma)$ for the SI/C_{14} solutions. Thus, $h_s(\gamma)$ and $h_{C_{14}}(\gamma)$ are similar not only in a qualitative sense (the M_{bI} and c_{bI} sensitivities explained above) but also in a quantitative sense. The SI/C_{14} solutions possess plasticity due to macrolattices of the micelles, and their nonlinear damping behavior quite possibly reflects large changes in the spatial position of the micelles due to the applied strain. Thus, the similarities between $h_s(\gamma)$ and $h_{C_{14}}(\gamma)$ suggests that the damping behavior of the slow process of the blends is also related to changes in the micelle position induced by the strain.

For the blends exhibiting complete relaxation, this effect of strain disappears and the terminal relaxation is achieved as the micelles undergo diffusion. This diffusion process would have a γ-insensitive terminal

relaxation time that is actually observed for the slow process of the micelles (cf. Figure 2). These results suggest that the slow process of the concentrated SI blends is related to the micelle diffusion, being in harmony with the discussion of part 1 for this process in the linear viscoelastic regime. However, no clear explanation has been obtained for the weaker γ dependence of h_s for the dilute micelles (Figure 14). This problem deserves further attention.

IV. Concluding Remarks

We have examined nonlinear damping behavior after imposition of the step strain for SI/I-4 micellar blends. The fast and slow processes characterizing the linear viscoelastic relaxation of the micelles were observed also for the nonlinear relaxation moduli $G(t,\gamma)$. The damping of $G(t,\gamma)$ was much more significant for the slow process than for the fast process, demonstrating the differences in the relaxation mechanisms of the two processes. For quantitative analysis, the $G(t,\gamma)$ data were separated into $G_f(t,\gamma)$ and $G_s(t,\gamma)$ for respective processes.

For $G_f(t,\gamma)$ for the fast process, the time−strain separability held at long time scales and the γ dependence of the damping function h_f agreed with that for homopolymer chains. This result indicates that the fast process of the micelles reflects the relaxation of *individual* corona I blocks, giving strong support for the discussion in part 1.

For the micelles exhibiting complete relaxation, $G_s(t,\gamma)$ for the slow process had γ-insensitive terminal relaxation times and obeyed the time−strain separability at long time scales. For concentrated micelles, the damping function for the slow process $h_s(\gamma)$ was close to the function $h_{C_{14}}(\gamma)$ for SI/C_{14} micellar solutions containing macrolattices. The nonlinear damping of these solutions is related to strain-induced changes in the position of the micelles. Thus, the similarity between $h_s(\gamma)$ and $h_{C_{14}}(\gamma)$ suggests that the slow, nonlinear relaxation process of the micelles in the SI/hI blends is also related to the changes in the micelle position and subsequent micelle diffusion having γ-insensitive relaxation times. This assignment is in harmony with the discussion of part 1. However, no clear explanation has been obtained for the weaker nonlinearity seen for the slow process of dilute micelles. Further studies are necessary for this problem.

References and Notes

(1) Sato, T.; Watanabe, H.; Osaki, K.; Yao, M.-L. *Macromolecules* **1996**, *29*, 3881 (preceding paper in this issue).
(2) Osaki, K.; Nishizawa, K.; Kurata, M. *Macromolecules* **1982**, *15*, 1068.
(3) Osaki, K.; Takatori, E.; Kurata, M.; Watanabe, H.; Yoshida, H.; Kotaka, T. *Macromolecules* **1990**, *23*, 4392.
(4) Osaki, K. *Rheol. Acta* **1993**, *32*, 429 and references therein.
(5) Menezes, E. V.; Graessley, W. W. *J. Polym. Sci., Polym. Phys. Ed.* **1982**, *20*, 1817.
(6) Pearson, D. S. *Rubber Chem. Technol.* **1987**, *60*, 439.
(7) Doi, M.; Edwards, S. F. *The Theory of Polymer Dynamics*; Clarendon: Oxford, U.K., 1986; Chapter 7.
(8) Takatori, E.; Osaki, K.; Kurata, M.; Hirayama, T. *J. Soc. Rheol. Jpn.* **1988**, *16*, 99.
(9) Watanabe, H.; Kotaka, T.; Hashimoto, T.; Shibayama, M.; Kawai, H. *J. Rheol.* **1982**, *26*, 153.
(10) Watanabe, H.; Kotaka, T. *Polym. J.* **1982**, *14*, 739.
(11) Watanabe, H.; Kotaka, T. *Polym. J.* **1983**, *15*, 337.
(12) Watanabe, H.; Kotaka, T. *J. Rheol.* **1983**, *27*, 223.
(13) Ferry, J. D. *Viscoelastic Properties of Polymers*, 3rd ed.; Wiley: New York, 1980; Chapter 4.

MA951844J